DOI: 10.1002/chem.200800250

Pyridine-Catalyzed Stereoselective Addition of Acyclic 1,2-Diones to Acetylenic Esters: Synthetic and Theoretical Studies of an Unprecedented Rearrangement

Abhilash N. Pillai,[a] Cherumuttathu H. Suresh,*[b] and Vijay Nair*[a]

Dedicated to Professor Gilbert Stork

Abstract: A systematic study of the addition of various 1,2-acyclic diones to activated acetylenic esters catalyzed by pyridine under mild conditions is described. This reaction provides a new protocol for the stereoselective synthesis of 1,2-diaroyl maleates. The exclusive formation of the *cis* isomer is especially noteworthy. This reaction occurs through the initial generation of a pyridine–dimethyl acetylene dicarboxylate zwitterion and its addition to the dione followed by an unprecedented benzoyl migration. Pyridine and substituted pyridines, such as 4-dimethylaminopyridine (DMAP) and 3-methoxypyridine, are the best catalysts and anhydrous 1,2-dimethoxyethane is found to be the solvent of choice. Structural, electronic, energetic and mechanistic details of the reaction are also revealed by density functional theory calculations, which strongly support the exclusive formation of the *cis* isomer of the 1,2-diaroyl maleates.

Keywords: diaroyl maleates · benzoyl migration · density functional calculations · pyridine catalysis · reaction mechanisms

Introduction

Carbon–carbon bond-forming reactions play a crucial role in organic synthesis. With the notable exception of pericyclic reactions, most carbon–carbon bond-forming processes involve the use of reactive intermediates, such as carbocations, carbanions, radicals and carbenes. It was realized that a class of potentially useful reactive intermediates, zwitterions, which are readily formed by the addition of nucleophiles to activated π-systems, although known for a long time,[1] have not found much use in organic synthesis, especially in carbon–carbon bond formation. In the context of our recent interest in multicomponent reactions involving zwitterions[2] formed from isoquinoline and dimethyl acetylenedicarboxylate (DMAD), we began exploring the reactions of the zwitterion formed from pyridine and DMAD; this species has a long history going back to the work of Diels and Alder[1a] in 1932, but its structure was established only three decades later by Acheson,[3] Winterfeldt[4] and Huisgen[5] independently.

It was found that the zwitterion **1** reacts readily with aromatic aldehydes (Scheme 1) to afford aroyl fumarates by a process tantamount to the *trans* addition of the aldehyde across the π system of the acetylenic ester.[6] Similar results were obtained in the reaction of the zwitterion **1**, formed in situ from pyridine and DMAD, with *N*-tosylimines[7] and electron deficient styrenes[8] (Scheme 2).

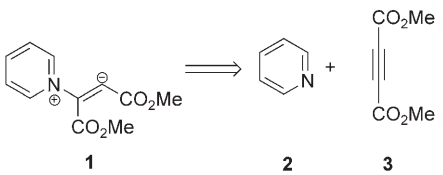

1 2 3

Scheme 1. Pyridine–DMAD zwitterion.

[a] Dr. A. N. Pillai, Prof. Dr. V. Nair
Organic Chemistry Section
National Institute for Interdisciplinary Science
and Technology (CSIR), Trivandrum-695019 (India)
Fax: (+91) 471-249-1712
E-mail: vijaynair_2001@yahoo.com

[b] Dr. C. H. Suresh
Computational Modelling and Simulation Section
National Institute for Interdisciplinary Science
and Technology (CSIR), Trivandrum-695019 (India)
Fax: (+91) 471-249-1712
E-mail: sureshch@gmail.com

Supporting information for this article is available on the WWW under http://www.chemeurj.org/ or from the author.

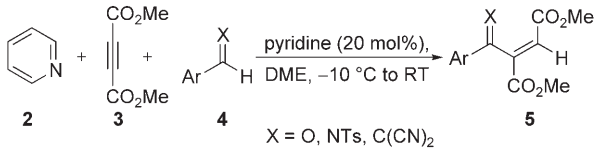

Scheme 2. Reaction of the pyridine–DMAD zwitterion with aldehydes, *N*-tosylimines and dicyanostyrenes.

This unprecedented reaction was impressive for the facility with which it occurred under very mild conditions (Scheme 2). The realization that the process involved the formal scission of the robust C–H bond of aryl aldehydes (BE $\approx$97 kcal mol^{-1}; BE = Bond energy) led us to surmise that a 1,2-dicarbonyl compound, such as benzil, with a relatively weak 1,2-C–C bond (BE $\approx$70 kcal mol^{-1}) was likely to engage in a reaction with the pyridine–DMAD zwitterion. In the event, a facile reaction leading to the formation of 1,2-dibenzoyl maleate occurred and the preliminary results have already been published.[9] Herein we report the details of work that involved the screening of several nucleophiles and solvents. Detailed computational studies aimed at gaining insight into the mechanistic pathway for the reaction are also included.

Results and Discussion

Synthetic studies: Our studies began with the addition of a catalytic amount (20 mol%) of pyridine to a solution of benzil **6** and DMAD (**3**) in anhydrous 1,2-dimethoxyethane (DME) at −10°C (Scheme 3). The reaction mixture was allowed to warm to room temperature ($\approx$30°C) and was then stirred for 8 h. The usual processing of the reaction mixture followed by column chromatography afforded dibenzoyl maleate **7** in 62% yield along with the unreacted benzil (33%).

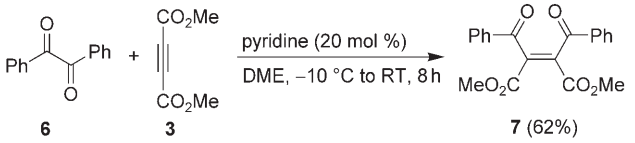

Scheme 3. Pyridine-catalyzed addition of DMAD to benzil.

Taking the reaction shown in Scheme 3 as the standard, several solvents were used instead of DME to examine whether there is any change in the efficiency of the reaction profile or the yield of product. The results of this study are summarized in Table 1 and clearly indicate that the reaction works well with polar solvents, which is presumably due to the stabilization of the zwitterion in polar solvents relative to non-polar solvents. Evidently, anhydrous DME is the solvent of choice.

A variety of nucleophiles were screened in place of pyridine, with the reaction of benzil and DMAD in anhydrous DME as the standard (Scheme 3) and the results are presented in Table 2. Interestingly, pyridine, 4-dimethylaminopyridine (DMAP) and 3-methoxypyridine afforded the best results.

Table 1. Effect of solvents.

Solvent	Conditions	Yield [%][a]
DME	−10°C→RT, 12 h	62 (92)
	reflux, 12 h,	63 (88)
THF	−10°C→RT, 12 h	44 (66)
	reflux, 12 h	48 (69)
CH_2Cl_2	−10°C→RT, 12 h	36 (61)
	reflux, 12 h	36 (61)
diethyl ether	−10°C→RT, 12 h	33 (53)
	reflux, 12 h	35 (54)
toluene	−10°C→RT, 12 h	39 (61)
	reflux, 12 h	42 (65)
cyclohexane	−10°C→RT, 12 h	24 (43)
	reflux, 12 h	25 (42)

[a] Yields based on recovered starting material are given in parentheses.

Table 2. Screening of catalysts.

Catalyst	Conditions	Yield [%][a]
pyridine	−10°C→rt, 12 h	62 (92)
	reflux, 12 h	63 (88)
DMAP	−10°C→rt, 12 h	65 (87)
	reflux, 12 h	67 (92)
3-methoxypyridine	−10°C→rt, 12 h	63 (90)
	reflux, 12 h	68 (92)
2-picoline	−10°C→rt, 12 h	33 (51)
	reflux, 12 h	33 (51)
2,6-lutidine	−10°C→rt, 12 h	< 10
	reflux, 12 h	< 10
triphenylphosphine	−10°C→rt, 12 h	0
	reflux, 12 h	0
triethyl amine	−10°C→rt, 12 h	0
	reflux, 12 h	0
DABCO	−10°C→rt, 12 h	0
	reflux, 12 h	0
DBU	−10°C→rt, 12 h	0
	reflux, 12 h	0
potassium *tert*-butoxide	−10°C→rt, 12 h	0
	reflux, 12 h	0

[a] Yields based on recovered starting materials are given in parentheses.

A dialkyl dione, 2,3-butanedione (**8**), also participated in the reaction with the pyridine–DMAD zwitterion under the usual conditions and product **9** was formed, albeit in low yields (Scheme 4). This may be due to side reactions that occur by deprotonation of the activated methyl groups of dione **8**.

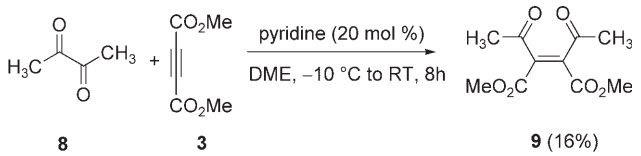

Scheme 4. Addition of DMAD to 2,3-butanedione catalyzed by pyridine.

To see if the size of the substituent in the ester group has any impact on the reactivity pattern, a reaction with di-*tert*-butyl acetylenedicarboxylate as the activated alkyne was carried out. The reaction proceeded smoothly in the same way as in the earlier cases to afford product **11** in 48% yield (Scheme 5), thus suggesting that the bulkiness of the ester group has no major effect on the yield of the product.

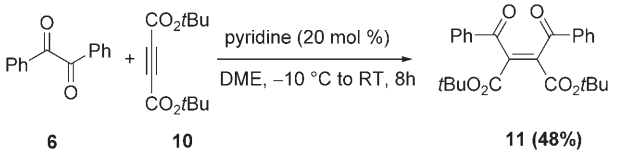

Scheme 5. Addition of di-*tert*-butyl acetylenedicarboxylate to benzil catalyzed by pyridine.

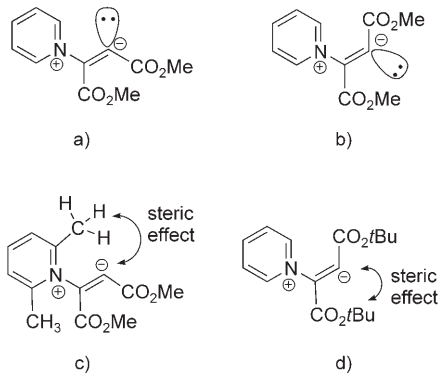

Figure 1. a) The active "*cis*" and b) the inactive "*trans*" form of **1** with the lone pair at the carbanion-like carbon atom. c) Steric effects in the 2,6-lutidine-derived zwitterion and d) the expected steric effect in the *trans* form of the zwitterion derived from di-*tert*-butyl acetylenedicarboxylate as the activated alkyne.

Electronic and steric effects: It should be noted that in Scheme 1 we have adopted a *cis* structure[10] (with respect to the ester moieties) for the zwitterionic intermediate **1**. Conceivably, the interaction of **1** with the electron-deficient dione is enhanced when the lone-pair centre at the carbanion-like carbon atom of **1** (Figure 1a) is more electron rich. The higher catalytic activity observed for DMAP and 3-methoxypyridine (Table 2) can be used as evidence in support of this electronic effect. Although the formation of a *trans* structure is also possible for this system (Figure 1b), on the basis of the following evidence, the existence of a *cis* structure can be confirmed as the active form. The first evidence came from the data obtained during the screening of catalysts (Table 2). As we can see, the catalytic efficiency of 2-picoline and 2,6-lutidine is less pronounced than that of pyridine, DMAP and 3-methoxypyridine. This suggests that steric interactions as presented in Figure 1c may be operative in *ortho*-substituted pyridines, which results in the shielding of the lone pair at the carbanion-like carbon atom, thus reducing its interaction with the dione. The *cis* form of the zwitterion is also supportive of the smooth reaction of di-*tert*-butyl acetylenedicarboxylate given in Scheme 5 because in such a configuration, the *t*Bu group is unable to exert a steric shielding effect on the lone-pair region of the active carbon atom. On the other hand, attribution of a *trans* structure to the zwitterion would have predicated it to lower reactivity towards di-*tert*-butyl acetylenedicarboxylate due to the presence of a steric shielding effect from the *t*Bu group in the lone-pair region of the active carbon (Figure 1d). Although the steric effect is in favor of the formation of the *cis* form of the zwitterion, the data in Table 2 do not fully eliminate the possibility of the formation of the *trans* form.

Mechanism: Two probable mechanistic pathways for the formal insertion of DMAD into benzil are depicted in Scheme 6.[9] In path 1, the zwitterion adds to one of the carbonyls of benzil to form an alkoxide intermediate **A**. The latter can transform into an epoxy derivative **B**, which then unravels to the pyridinium ylide **C**. It is conceivable that intramolecular benzoyl transfer followed by elimination of pyridine can afford the final product. In path 2, a 1,2-migration of the benzoyl anion in **A** to form a pyridinium ylide **E** and subsequent generation of a cyclopropane intermediate **F** is conceived. Elimination of pyridine from **F** furnishes the product.

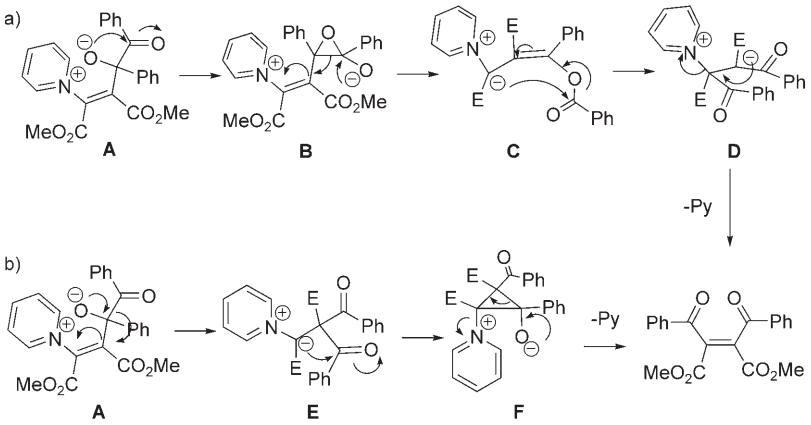

Scheme 6. Proposed mechanistic rationalization for the reaction. a) Path 1, b) path 2; Py = pyridine

To obtain support for the postulated reaction mechanism, we resorted to theoretical calculations by using DFT. DFT methods have been accepted as efficient and reasonably ac-

curate methods and they have become a powerful tool in transition-state modelling, particularly for ground-state reactions.[11,12] We have selected the reaction of 2,3-butanedione with DMAD and pyridine (Scheme 4) for the theoretical study. Details of these calculations are discussed in the following section.

Theoretical calculations: All the molecular geometries were optimized at the DFT level by using Becke's three-parameter exchange functional in conjunction with the Lee–Yang–Parr correlation functional (B3LYP)[13] as implemented in the Gaussian 03 suite of programs.[14] For H, C, N and O atoms, the 6-31G(d) basis functions were selected for solving the Schrödinger equation.[15] Normal coordinate analysis has been performed to characterise all the stationary points. The energy-minimum structures showed positive eigenvalues of the Hessian matrix, whereas transition states (TSs) showed one negative eigen value. All the transition states were computed by using the Transit-Guided Quasi-Newton (STQN;QST3) method.[16,17] For most TSs, the analysis including the visualization of the negative frequency was sufficient to specify the corresponding reaction path. In the case of **TS2**, intrinsic reaction coordinate (IRC) calculations near the TS region followed by geometry optimisation of both reactants and products were performed to confirm its connectivity to reactant and product.[18] Zero-point energy (ZPE), entropy corrections, thermal correction to enthalpy, and thermal correction to Gibbs free energy were derived by using unscaled frequencies and the usual approximations of statistical thermodynamics (ideal gas, harmonic oscillator and rigid rotor) at a temperature of 298.15 K and a pressure of 1.00 atm. Furthermore, the solvation free-energy values ($E_{solvation}$) along the reaction coordinate were evaluated from the self-consistent reaction field (SCRF) procedure.[19] All of the solvation calculations were performed at the B3LYP/6-311++G(2d,2p) level by using the geometries optimised at the B3LYP/6-31G(d) level in the gas phase. The selected SCRF procedure is the polarisable continuum model (PCM) by using Klamt's form of the conductor reaction field (COSMO).[19–22] The standard state of a solution is taken as 1 mol L^{-1} at 298.15 K, and an additional correction to the free-energy terms is needed to convert the standard state of an ideal gas ($P0=1$ atm) to the standard state of the solution ($c0=1$ mol L^{-1}) and this was obtained by adding the term $RT\ln(RT)$ to each free energy term (the value of this correction is 1.8943 kcal mol^{-1} at 298.15 K). The relative Gibbs free-energy values in the standard state of 1 mol L^{-1} suitable for solution reactions have been used throughout the text to describe the energetics. For zwitterionic systems, the electron-localization features were explored by analyzing their molecular electrostatic potential (MESP) at the B3LYP/6-31G(d) level.[23–25]

Electronic features of pyridine, diester, and dione and the formation of pyridine–dione and pyridine–diester adducts: In the diester, the ester groups are in an orthogonal arrangement whereas in the dione, the carbonyl groups prefer a *trans* arrangement. The C_{sp2}–C_{sp2} length of 1.550 Å in the dione is unusually long for a bond between sp^2-hybridized carbon atoms, which suggests its electron deficiency due to the localization of carbonyl groups. In pyridine, the nitrogen lone pair is the HOMO, which indicates its nucleophilic character. Attractive electrostatic interactions arise when the pyridine nitrogen atom approaches the electron deficient C_{sp2}–C_{sp2} bond of the dione, which in turn leads to the formation of a weak pyridine–dione complex (**12**). The enthalpy change ΔH (enthalpy of product−enthalpy of reactant) accompanying this associative reaction is found to be −3.2 kcal mol^{-1}, whereas the free-energy change ΔG at the B3LYP/6-31G(d) level has a positive value of 3.2 kcal mol^{-1} due to the negative entropy factor. Furthermore, activation of the C_{sp2}–C_{sp2} bond of the dione in **12** is expected to lead to the formation of the pyridine–dione covalent adduct containing a N–C bond. However, all attempts to optimise the adduct structure resulted in the formation of the weak complex **12** (Figure 2). If such an adduct is formed, the negative

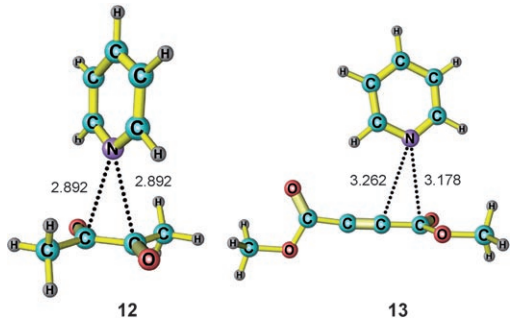

Figure 2. Pyridine–dione and pyridine–diester complexes. Bond lengths are given in angstroms [Å].

charge will be localized on the dione oxygen due to its connectivity to the newly forming sp^3 carbon atom, a situation quite unfavourable for thermodynamic stability. Therefore, the pyridine–dione interaction is irrelevant from a mechanistic point of view.

Similar to the pyridine–dione complex, pyridine–diester complex **13** is formed when the pyridine nitrogen atom is attracted towards the ester group of the diester (Figure 2). This complex formation is exothermic by 1.6 kcal mol^{-1}, whereas the negative entropy factor gives an endergonic value of 4.4 kcal mol^{-1} at the B3LYP/6-31G(d) level.

Zwitterionic complexes: From **13**, a zwitterionic complex **14** (Figure 3a) is formed when the pyridine nitrogen interacts covalently with the acetylenic triple bond. This can even be considered as the Michael-type addition of the nitrogen atom of pyridine to one of the two conjugated positions of DMAD. Complex **14** is a Huisgen zwitterion-type species and similar species have been proposed as intermediates in polar cycloaddition reactions.[12a] In complex **14**, the ester groups are in a *cis* arrangement with respect to the C=C

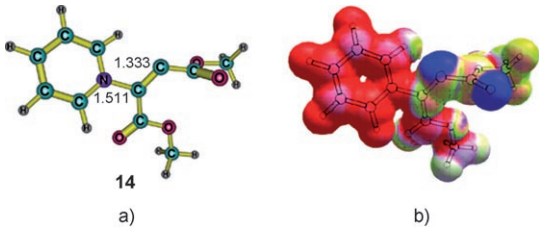

Figure 3. a) Pyridine–diester zwitterionic adduct **14**. Bond lengths are given in angstroms [Å]. b) MESP pasted on the van der Waals surface of **14**. The color coding from blue to red is −10.0 to +60.0 kcal mol^{-1}.

double bond (a *trans* arrangement of the ester groups is less stable than the *cis* arrangement by 2.0 kcal mol^{-1}). The MESP picture of **14** (Figure 3b) gives a clear idea of its zwitterionic character, wherein the pyridine ring is positively charged (red region) and the negatively charged carbon atom (blue region) is evident on the DMAD moiety. A MESP minimum value of −61.9 kcal mol^{-1} is observed for this carbon atom, which is nearly equal to the MESP minimum value calculated for pyridine (−62.4 kcal mol^{-1}); this clearly suggests that the DMAD moiety possesses the character of a stabilised carbanion. Therefore, a high nucleophilic reactivity in the σ-plane is expected for the negatively charged carbon atom (blue region in Figure 3b), whereas the π-delocalization of the positive charge through the ring atoms and the connected ester moiety (red region mainly centred on the pyridine ring and ester moiety) contributes towards its stability.

It can be noted that the formation of **14** from free pyridine and diester is endothermic by 10.4 kcal mol^{-1}. Because it is an association reaction, the entropy factor is negative and, therefore, a high value for the free-energy change (22.3 kcal mol^{-1}) is observed, which suggests that the thermodynamic factors are not very favourable for the reaction in the gas phase and the observed formation of complex **14** in the experiment can be explained by invoking solvation effects and kinetic factors. Therefore, **14** is expected to be a highly reactive short-lived zwitterionic intermediate. The experiments conducted in the present work and the previous reports on similar reactions are in favour of the above-mentioned observation.

The nucleophilic attack of Huisgen zwitterion **14** by its carbanion on the electron deficient carbonyl carbon atoms of the dione is considered as the next step of the reaction and this would lead to the formation of zwitterionic complex **15** (Figure 4). Energetically, complex **15** is quite stable as its formation from **14** and dione is exothermic by 7.9 kcal mol^{-1}, whereas the free energy of the reaction shows a decrease by 1.5 kcal mol^{-1}. It can be noted that with respect to the electronic energy, enthalpy and free energy of (pyridine + dione + diester), the corresponding relative values of **15** are −0.5, 2.5 and 23.8 kcal mol^{-1}, respectively. The free-energy change observed for **15** in the gas phase is quite large as it is built from three small molecules. By starting from complex **15**, two mechanistic possibilities will be discussed.

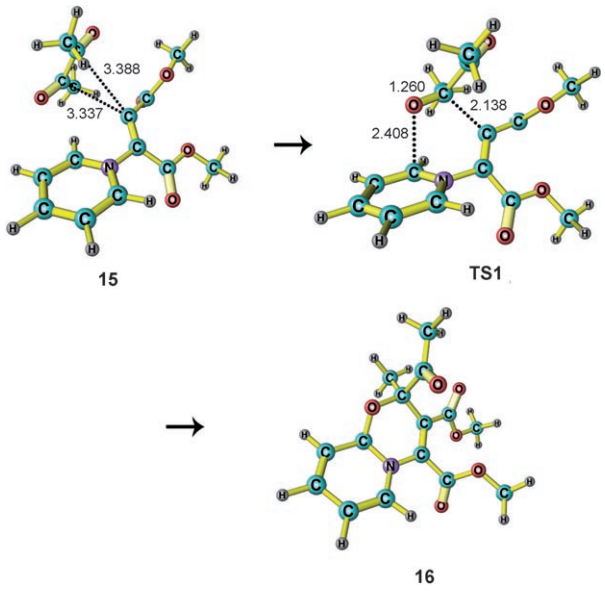

Figure 4. 1,4-dipolar cycloaddition. Bond lengths are given in angstroms [Å].

Mechanism 1: In the reactant complex **15**, a further approach of the dione to the negatively charged carbon atom in the zwitterion is expected to produce a C–C bond between the two moieties. However, a transition state (TS) located for this process produced the structure **TS1** (Figure 4), which showed simultaneous formation of a C–C and C–O bond. The structure of **TS1** is quite similar to a TS typically observed in a cycloaddition reaction and the present case may be better described as resulting from a 1,4-dipolar cycloaddition. The free energy of activation ($\Delta G^{\#}$) for this step is only 8.3 kcal mol^{-1} and the free energy of product **16** was found to be 18.2 kcal mol^{-1} lower than **15**. It can be noted that in **15**, the pyridine moiety carries a positive charge and when the C–C bond starts to develop in **TS1** at 2.138 Å (see the structure of **TS1**), the negative charge will be transferred to the carbonyl group of the dione moiety and, correspondingly, the activation of this C–O bond (1.260 Å in **TS1**) will occur. Hence, in **TS1** there is a favourable electrostatic interaction between the negatively charged dione oxygen atom and the positively charged pyridine moiety. This may be the reason for the low activation barrier for this reaction. Similar electrostatic stabilisation was reported recently for a zwitterionic transition state corresponding to the formation of a 1,3-dipolar cycloadduct of bis-(phenylazo)stilbene.[24a] Compared to **TS1**, the charge is well balanced in **16** and it is a normal neutral molecule, in which the nitrogen shows a slight amount of pyramidalization. It can be noted that the loss of aromaticity in the pyridine ring of **16** is well compensated by the formation of two new bonds, which accounts for the high exothermicity of this step of the reaction. We have also determined the structure of transition-state **TS1** in the solvent phase (solvent = THF) by using the PCM method and it is found that gas phase structure is nearly preserved in solution (see the Supporting

Information). In other words, the formation of a zwitterionic complex that would be more stable than the neutral bicyclic compound **16** is not observed.[12e]

A structure similar to intermediate **16** was isolated in an earlier work, in which the pyridine–DMAD zwitterion was intercepted with N-substituted isatins,[7] which supports the mechanism discussed so far. Further rearrangement of the intermediate **16** is anticipated and the possibility of the breaking of the newly formed C–O bond is assessed by locating **TS2** (Figure 5). It can be seen that in **TS2**, the oxygen

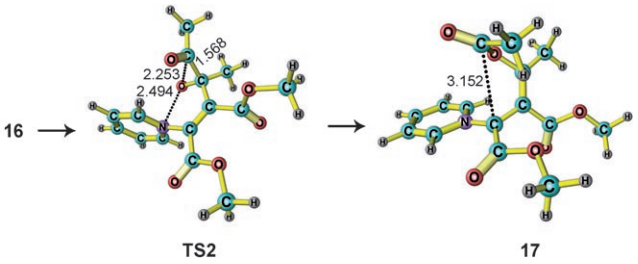

Figure 5. C–O bond breaking leading to a zwitterionic intermediate. Bond lengths are given in angstroms [Å].

atom disconnected from the pyridine ring interacts with the C–C bond of the dione moiety at a distance of 2.253 Å. In this TS, the original dione C–C bond is further activated to a distance of 1.568 Å. The product from **TS2** is expected to be an epoxide. However, the geometry optimisation produced the structure **17**, in which the original dione C–C bond is found to be completely cleaved. The **16** to **17** conversion required a $\Delta G^{\#}$ of 26.9 kcal mol^{-1} and this process is exergonic by 9.6 kcal mol^{-1}.

It can be noted that in **17**, the pyridine ring carries a positive charge, which means that it is zwitterionic in nature. Further, **17** is 9.6 kcal mol^{-1} more stable than **16**. The energetic stabilisation is interesting because normally a charge separated system is expected to be less stable than its neutral isomer. In **17**, we can see two ester groups and one $-OCOCH_3$ group, and each of these groups is connected to a different sp^2 carbon atom. This means that a major share of the negative charge of the zwitterion can delocalise over all of these groups via the sp^2 carbon atoms and the connected oxygen atoms. From the bond-length features of **17**, it is felt that the carbon atom connected to the nitrogen atom is exposed to more electron density because the three bonds on this carbon atom are more like single bonds. Therefore, the C···C distance of 3.152 Å noted in the structure of **17** is expected to be the next hot region for a chemical change. This is indeed true because at the C···C distance of 2.138 Å, **TS3** is located, which yields complex **18** (Figure 6). Compared to **17**, complex **18** is further stabilized

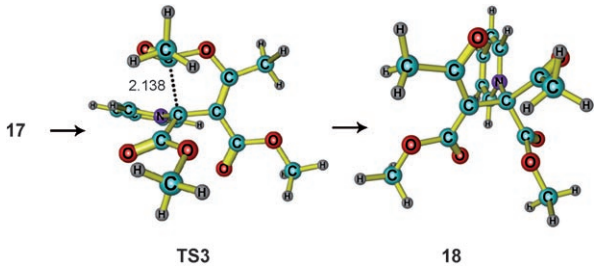

Figure 6. C–O bond breaking leading to $-COCH_3$ migration. Bond lengths are given in angstroms [Å].

by 3.0 kcal mol^{-1} in free energy. The **17** to **18** conversion is the result of a C–O bond breaking that leads to the migration of the $CH_3C{=}O$ group. The $\Delta G^{\#}$ of this step is only 4.4 kcal mol^{-1}. The dissociation of pyridine from **18** is expected to be spontaneous as it releases 16.4 kcal mol^{-1} of energy, which leads to the formation of the desired *cis*-1,2-dialkoyl enoate **19**.

The reaction profile, which shows the changes of enthalpy, free energy and $E_{solvation}$ is depicted in Figure 7.[26] The overall reaction is highly exothermic and exergonic and the rate-determining step corresponds to the conversion of the bicy-

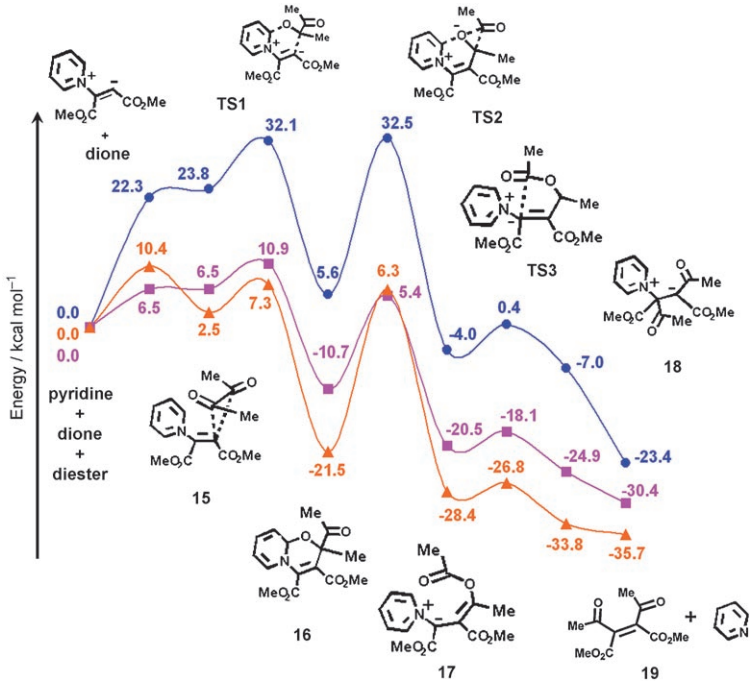

Figure 7. Relative Gibbs free-energy values in the gas phase (●) and PCM level relative $E_{solvation}$ values (■) obtained for mechanism 1. The relative enthalpy profile in the gas phase is also given (▲).

clic intermediate **16** to the open system **17**. Solvation plays an important role as it gives more stability to transition states relative to other minimum-energy structures. The solvation effect is the largest for the transition-state **TS2** located for the rate-determining step and this in turn reduces the activation barrier to a feasible value of 16.1 kcal mol^{-1}.

Mechanism 2: We have also considered the possibility of the migration of the $-COCH_3$ group in **16** to the nearby sp^2 carbon atom. **TS4** was located for this process, which yields the 1,2-migration product **20** (Figure 8). The $\Delta G^{\#}$ of this step is 27.2 kcal mol^{-1}, which is only 0.3 kcal mol^{-1} higher in energy than the **16** to **17** conversion discussed in mechanism 1. Furthermore, the **16** to **20** conversion is endergonic by 3.0 kcal mol^{-1}, whereas the **16** to **17** conversion is exergonic by 9.6 kcal mol^{-1}. From **20**, migration of the $-COCH_3$ group to the sp^2 carbon connected to the nitrogen atom is also feasible as a TS located for such a reaction (**TS5**) required only a $\Delta G^{\#}$ value of 16.8 kcal mol^{-1} (Figure 8). The product obtained from **TS5** is the same compound **18** already located in mechanism 1. The reaction profile depicted in Figure 9 also suggests that even in the presence of solvent, this reaction required the highest activation energy of 24.3 kcal mol^{-1} (conversion of **16** to **20** through **TS4**).

It can be noted that **TS2** of mechanism 1 yields a more stable intermediate (**17**) than that which results from **TS4** of mechanism 2 (**20**). The conversion of **17** to the final product **19** is more facile than the conversion of **20** to **19** because the former required an activation energy of only 2.4 kcal mol^{-1} compared with 11.3 kcal mol^{-1} for the latter (solvent phase values). The solvation effect is clearly in favour of mechanism 1 as the rate determining step, which shows an activation barrier of 16.1 kcal mol^{-1} that is 8.2 kcal mol^{-1} smaller than the corresponding value obtained for mechanism 2 (solvent phase). Furthermore, if we follow mechanism 2, the dissociation of **16** to the starting materials is found to be easier than the formation of intermediate **20**. On the basis of the above results, it can be concluded that mechanism 1 is preferred over the competitive mechanism 2 in both the gas and solvent phases.

Molecular dynamics calculations: Although our experiments and related studies in the literature[10] strongly support the formation of the zwitterion **14** as a transient species, the credibility of the reported theoretical results depends on the existence of complex **14** in the system. Although the gas-phase relative free energy of 22.1 kcal mol^{-1} observed for this system is rather high, the relative $E_{solvation}$ value of 6.5 kcal mol^{-1} supports the formation of this species in the reaction mixture. The high solvation effect is observed because of the zwitterionic character of the molecule. To gain further support for this argument, we have analyzed the kinetic stability of **14** by simulated annealing techniques that involve semiempirical Born–Oppenheimer molecular dynamics (BOMD) calculations at the PM3 level.[27] The simulations were done for 1155 fs at a simulated temperature of 273 K. The default criteria used in the Gaussian 03 pro-

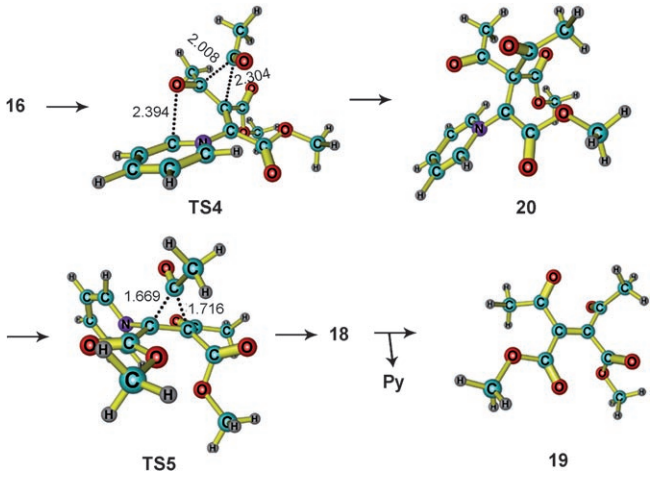

Figure 8. Mechanism 2 showing the 1,2-migrations of $-COCH_3$. Bond lengths are given in angstroms [Å].

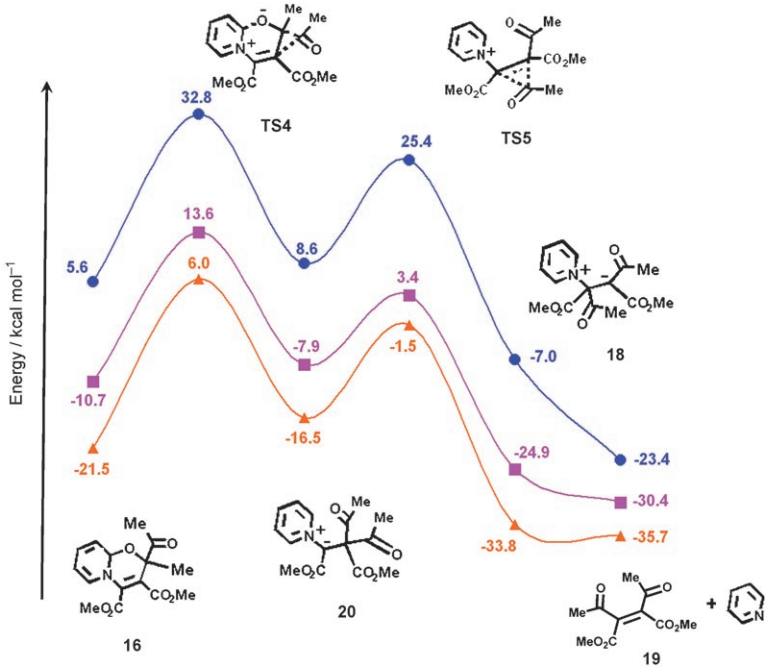

Figure 9. Relative Gibbs free-energy values in the gas phase (●) and PCM level relative $E_{solvation}$ values (■) obtained for mechanism 2. The relative enthalpy profile in the gas phase is also given (▲).

gram[14] were used for setting up the initial conditions. At about 1100 fs, the complex dissociated to pyridine and diester units (Figure 10). Interestingly, the simulation also showed the migration of a proton from the pyridine ring to the negatively charged carbon atom (see the model shown in the middle of Figure 10). The product from the proton migration retained its structure for around 70 fs. The proton migration was also studied at the B3LYP/6-31G(d) level, which confirmed that the migration can take place with an activation energy of 14.5 kcal mol^{-1} and the product of the reaction was 4.8 kcal mol^{-1} less stable than **14**.

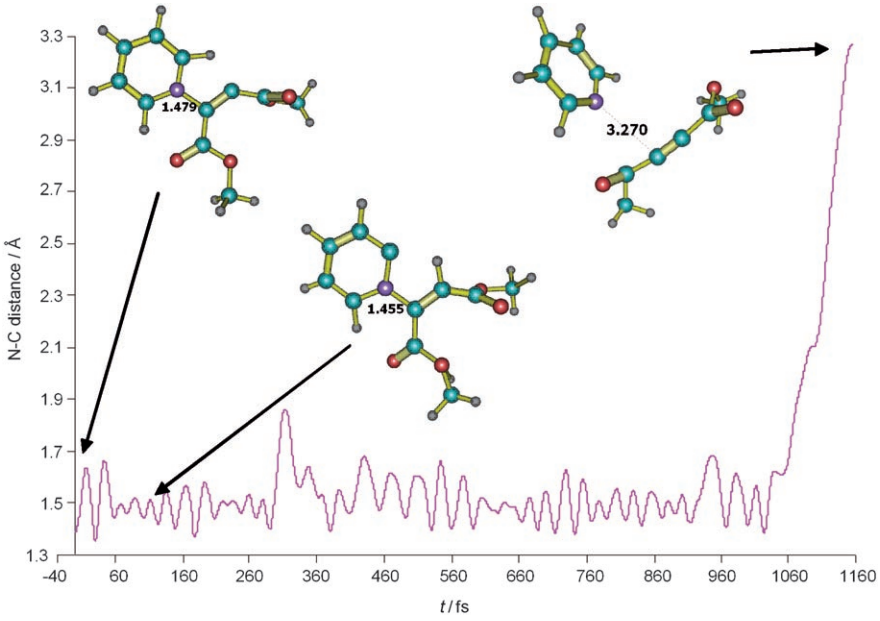

Figure 10. BOMD simulation showing the histogram of the C–N bond lengths. A proton is seen to migrate from the pyridine ring to the negatively charged carbon atom after 70 fs. C–N bond lengths indicated are a) 3.370, b) 1.455 and c) 1.479 Å.

The BOMD calculations are rather computationally expensive and more sophisticated ab initio or DFT simulations were unaffordable. The results of the PM3 level BOMD simulation support at least a 1 ps lifetime for the zwitterion system **14**. The proton migration in **14** indicates the high reactivity of its negatively charged carbon atom. The proton migration may be advantageous for the reaction because it would increase the concentration of the active species in the reaction mixture by preventing the quick dissociation of the C–N bond.

On comparing the mechanistic postulates proposed with those from theoretical calculations, the following conclusions can be made. The experimental results and theoretical calculations support the proposed formation of the zwitterion **14** between pyridine and DMAD as the initial step. The BOMD simulation strongly suggests that **14** is a highly reactive species with a short lifetime in the order of pico seconds. Instead of the zwitterion **A** as proposed in the mechanistic postulate (Scheme 6), the formation of an adduct **16** between the zwitterion, generated from pyridine and DMAD, and the dione is located by calculations (Figure 4). The bicyclic adduct **16** is a locked system and the breaking of the new C–O bond can only happen in such a way that it will lead to the *cis* product. This is validated as the product formed is exclusively the *cis* isomer. Similarly, in place of epoxy derivative **B**, a transition-state **TS2** is found in which the C–C and C–O bonds are partially broken; this TS then proceeds to **17** (**C** in Scheme 6) in which the original C–C dione bond is completely cleaved. Then, the acyl-group migration takes place by the breaking of the C–O bond (**18** or **D**) followed by elimination of pyridine to give the products, which are similar in both the suggested postulates and calculations.

In the second postulated mechanism, the key intermediate in the calculation is also the adduct **16**. From **16**, a 1,2-acyl migration occurs which gives the intermediate **20** (**E**). Instead of the cyclopropane system **F** in the proposed mechanism (Scheme 6), the transition state **TS5** is located by calculations in which simultaneous breaking of one C–C bond and formation of another C–C bond is observed. The rest are the same in both the postulate and the calculation. But the theoretical results predict that mechanism 1 is preferred.

It can be noted that with respect to the central C–C bond of **18**, the ester groups have a *cis* arrangement and, therefore, the dissociation of pyridine from **18** would give the *cis* product **19**. However, considering the single-bond character of the central C–C bond, there exists the possibility of the rotation of this bond leading to the formation of a *trans*-structure. The B3LYP/6-31G(d) level calculations showed a value of 10.0 kcal mol^{-1} for the rotation of the C–C bond for the formation of the *trans* isomer of **18**, which was 0.7 kcal mol^{-1} less stable than the *cis* form (see the Supporting Information). Thus the thermodynamics are in favour of the formation of *cis* product **19**.

Conclusion

We have uncovered a novel reaction, in which acyclic 1,2-diones add to an activated acetylene providing a unique synthetic protocol for the stereoselective synthesis of 1,2-diaroyl maleates. The screening of various catalysts showed that pyridine and substituted pyridines act as mediators for C–C

bond formation in these reactions. It was also shown that the reaction works well with pyridine, 4-dimethylaminopyridine (DMAP) and 3-methoxypyridine. A detailed study with various solvents has shown that the reaction works well in anhydrous 1,2-dimethoxyethane. It is noteworthy that the reaction occurs by means of an unprecedented benzoyl/acyl migration. The structural, electronic, energetic and mechanistic details of the reaction are also unravelled by theoretical calculations, which strongly supported the exclusive formation of the *cis* isomer, relative to 1,2-diaroyl maleates. The negatively charged carbon atom of the transient species, *cis*-zwitterion **14**, was identified as the reactive centre that upon coordination to the dione gives the fairly stable intermediate product **16**. This means that the transformation of the transient species **14** to the stable intermediate **16** drives the reaction in the forward direction. As we can see from mechanism 1 (Figure 7), once **16** is formed, its decomposition to **14** and dione is less-favoured relative to the formation of **17** as the former process is endergonic, whereas the later one is exergonic. Furthermore, the forward reaction from **16** is more facile than the backward reaction. The stereochemistry of the product **19** is thus mainly decided at the beginning, when **16** is formed from the *cis* zwitterion. Although the rotation of the central C–C bond in **18** can give rise to a *trans* isomer of **19**, the rotation itself requires an activation energy of 10.0 kcal mol^{-1} and, therefore, the predominant formation of the *cis* isomer **19** is expected. The solvent effect plays a major role in the facile formation of the products as there is a substantial reduction in the activation barrier in all steps of the reaction, which is mainly attributed to the increased stability of the highly charge-separated transition states in the solvent phase.

Experimental Section

General information: Melting points were recorded on a Buchi melting point apparatus and are uncorrected. NMR spectra were recorded at 300 (^{1}H) and 75 MHz (^{13}C), respectively, on a Bruker Avance DPX-300 MHz NMR spectrometer. Chemical shifts are reported (δ) relative to TMS (^{1}H) and $CDCl_3$ (^{13}C) as the internal standards. Coupling constants (J) are reported in hertz (Hz). Mass spectra were recorded under EI/HRMS (at 5000) resolution by using an Auto Spec. mass spectrometer. IR spectra were recorded on Bomem MB Series FTIR spectrophotometer. Elemental analyses were performed on Perkin–Elmer 2400 Elemental Analyzer.

Dimethyl (2*Z*)-2,3-dibenzoylbut-2-enedioate (7): Pyridine (20 mol %) was added to a solution of benzil **6** (100 mg, 0.4762 mmol) and DMAD (**3**) (82 mg, 0.5714 mmol) at −10 °C. The reaction mixture was allowed to attain room temperature and was then stirred for 8 h. The solvent was distilled off in vacuo by using a rotary evaporator, followed by column chromatography as described in the general procedure to afford the product **7** as a white crystalline solid (101 mg, 62 %). M.p.: 138–140 °C (recrystallized from a CH_2Cl_2/hexane mixture); ^{1}H NMR: δ = 7.80 (d, J = 7.34 Hz, 4H), 7.56 (t, J = 7.46 Hz, 2H), 7.41 (d, J = 7.78 Hz, 4H), 3.81 ppm (s, 6H); ^{13}C NMR: δ = 189.9, 163.7, 141.6, 135.3, 134.2, 129.5, 128.7, 53.3 ppm; IR (KBr): $\tilde{\nu}$ = 2961, 1754, 1666, 1592, 1448, 1430, 1132 cm^{-1}; elemental analysis calcd (%) for $C_{20}H_{16}O_6$: C 68.18, H 4.58; found: C 68.32, H 4.52.

Dimethyl (2*Z*)-2,3-diacetylbut-2-enedioate (9): Pyridine (20 mol %) was added to a solution of 2,3-butanedione (**8**) (100 mg, 1.1628 mmol) and DMAD (**3**) (198 mg, 1.3953 mmol) at −10 °C. The reaction mixture was allowed to attain room temperature and was then stirred for 12 h. Removal of the solvent followed by column chromatography as described in the general procedure afforded product **9** as a viscous yellow liquid (43 mg, 16 %). ^{1}H NMR: δ = 3.86 (s, 6H), 2.24 ppm (s, 6H); ^{13}C NMR: δ = 189.5, 165.1, 134.6, 44.0, 28.5 ppm; IR (KBr): $\tilde{\nu}$ = 2967, 1743, 1682, 1564, 1441, 1351, 1132 cm^{-1}; HRMS (EI): m/z: calcd for $C_{10}H_{12}O_6$: 228.0634 [M^+]; found: 228.0663.

Di-*tert*-butyl (2*Z*)-2,3-dibenzoylbut-2-enedioate (11): Pyridine (20 mol %) was added to a solution of benzil **6** (100 mg, 0.4762 mmol) and di-*tert*-butyl acetylenedicarboxylate **10** (129 mg, 0.5714 mmol) at −10 °C. The reaction mixture was allowed to attain room temperature and was then stirred for 12 h. Removal of the solvent followed by column chromatography afforded product **11** as a crystalline white solid (110 mg, 48 %). M.p.: 145–147 °C (recrystallized from a CH_2Cl_2/hexane mixture); ^{1}H NMR: δ = 8.01 (d, J = 7.32 Hz, 4H), 7.58–7.51 (m, 6H), 1.14 ppm (s, 18H); ^{13}C NMR: δ = 191.2, 161.8, 142.2, 136.0, 133.7, 128.9, 128.7, 27.3 ppm; IR (KBr): $\tilde{\nu}$ = 2943, 1751, 1672, 1579, 1443, 1406, 1126 cm^{-1}; HRMS (EI): m/z: calcd for $C_{26}H_{28}O_6$: 436.1886 [M^+]; found: 436.1904.

Acknowledgements

We thank the Council of Scientific and Industrial Research (CSIR) and Department of Science and Technology (DST), New Delhi for financial assistance. We also thank S. Mathew for the spectral data and S. Viji for all the mass and elemental analysis.

[1] a) O. Diels, K. Alder, *Liebigs Ann. Chem.* **1932**, *498*, 16; b) R. M. Acheson, *Adv. Heterocycl. Chem.* **1963**, *1*, 125; c) E. Winterfeidt, *Angew. Chem.* **1967**, *79*, 389; *Angew. Chem. Int. Ed. Engl.* **1967**, *6*, 423.
[2] V. Nair, C. Rajesh, A. U. Vinod, S. Bindu, A. R. Sreekanth, J. S. Mathen, L. Balagopal, *Acc. Chem. Res.* **2003**, *36*, 899.
[3] R. M. Acheson, A. O. Plunkett, *J. Chem. Soc.* **1964**, 2676.
[4] E. Winterfeldt, *Chem. Ber.* **1965**, *98*, 3537.
[5] R. Huisgen, M. Morikawa, K. Herbig, E. Brunn, *Chem. Ber.* **1967**, *100*, 1094.
[6] a) V. Nair, A. R. Sreekanth, A. U. Vinod, *Org. Lett.* **2001**, *3*, 3495; b) V. Nair, A. R. Sreekanth, A. U. Vinod, *Org. Lett.* **2002**, *4*, 2807.
[7] V. Nair, A. R. Sreekanth, N. Abhilash, A. T. Biju, B. Remadevi, R. S. Menon, N. P. Rath, R. Srinivas, *Synthesis* **2003**, 1895.
[8] V. Nair, B. Remadevi, N. Vidya, R. S. Menon, N. Abhilash, N. P. Rath, *Tetrahedron Lett.* **2004**, *45*, 3203.
[9] V. Nair, A. N. Pillai, R. S. Menon, E. Suresh, *Org. Lett.* **2005**, *7*, 1189.
[10] Indirect evidence for the *cis* configuration of the zwitterion was accrued from literature reports,[1,3] which show that the zwitterion **1** adds to another molecule of acetylenic ester to form a second zwitterion, which then cyclizes to form 4*H*-quinolizine. Evidently the addition product from a transoid zwitterion would not undergo such a cyclization.
[11] a) J. M. Seminario, P. Politzer, *Modern Density Functional Theory. A Tool for Chemistry*, Elsevier, Amsterdam, **1995**; b) K. N. Houk in *1,3-Dipolar Cycloaddition Chemistry* (Ed:. A. Padwa), *Vol. 2*, Wiley, New York, **1984**; c) C. F. Christian, T. Takeya, M. J. Szymanski, D. A. Singleton, *J. Org. Chem.* **2007**, *72*, 6183; d) D. A. Singleton, S. R. Merrigan, *J. Am. Chem. Soc.* **2000**, *122*, 11035; e) M. H. El-Badri, D. Willenbring, Tantillo, D. J. Gervay-Hague, *J. Org. Chem.* **2007**, *72*, 4663.
[12] a) L. R. Domingo, M. Arnó, R. Contreras, P. Pérez, *J. Phys. Chem. A* **2002**, 106, 952; b) L. R. Domingo, *Eur. J. Org. Chem.* **2004**, *23*, 4788; c) L. R. Domingo, M. T. Picher, *Tetrahedron* **2004**, *60*, 5053; d) M. J. Aurell, L. R. Domingo, P. Pérez, R. Contreras, *Tetrahedron* **2004**, *60*, 11503; e) L. R. Domingo, M. T. Picher, J. Andrés, V. Moliner, V. S. Safont, *Tetrahedron* **1996**, *52*, 10693.

[13] a) A. D. Becke, *J. Chem. Phys.* **1993**, *98*, 5648; b) A. D. Becke, *Phys. Rev. A* **1988**, 38, 3098; c) C. T. Lee, W. T. Yang, R. G. Parr, *Phys. Rev. B* **1988**, *37*, 785.
[14] Gaussian 03, Revision C.02, M. J. Frisch, G. W. Trucks, H. B. Schlegel, G. E. Scuseria, M. A. Robb, J. R. Cheeseman, J. A. Montgomery, Jr., T. Vreven, K. N. Kudin, J. C. Burant, J. M. Millam, S. S. Iyengar, J. Tomasi, V. Barone, B. Mennucci, M. Cossi, G. Scalmani, N. Rega, G. A. Petersson, H. Nakatsuji, M. Hada, M. Ehara, K. Toyota, R. Fukuda, J. Hasegawa, M. Ishida, T. Nakajima, Y. Honda, O. Kitao, H. Nakai, M. Klene, X. Li, J. E. Knox, H. P. Hratchian, J. B. Cross, V. Bakken, C. Adamo, J. Jaramillo, R. Gomperts, R. E. Stratmann, O. Yazyev, A. J. Austin, R. Cammi, C. Pomelli, J. W. Ochterski, P. Y. Ayala, K. Morokuma, G. A. Voth, P. Salvador, J. J. Dannenberg, V. G. Zakrzewski, S. Dapprich, A. D. Daniels, M. C. Strain, O. Farkas, D. K. Malick, A. D. Rabuck, K. Raghavachari, J. B. Foresman, J. V. Ortiz, Q. Cui, A. G. Baboul, S. Clifford, J. Cioslowski, B. B. Stefanov, G. Liu, A. Liashenko, P. Piskorz, I. Komaromi, R. L. Martin, D. J. Fox, T. Keith, M. A. Al-Laham, C. Y. Peng, A. Nanayakkara, M. Challacombe, P. M. W. Gill, B. Johnson, W. Chen, M. W. Wong, C. Gonzalez, J. A. Pople, Gaussian, Inc.: Wallingford CT, **2004**.
[15] a) W. R. Wadt, P. J. Hay, *J. Chem. Phys.* **1985**, *82*, 284; b) P. J. Hay, W. R. Wadt, *J. Chem. Phys.* **1985**, *82*, 299.
[16] C. Peng, P. Y. Ayala, H. B. Schlegel, M. J. Frisch, *J. Comput. Chem.* **1996**, *17*, 49.
[17] C. Peng, H. B. Schlegel, *Isr. J. Chem.* **1993**, *33*, 449.
[18] a) C. González, H. B. Schlegel, *J. Chem. Phys.* **1991**, *95*, 5853; b) K. Fukui, *Acc. Chem. Res.* **1981**, *14*, 363.
[19] a) J. Tomasi, M. Persico, *Chem. Rev.* **1994**, *94*, 2027; b) C. J. Cramer, D. G. Truhlar, *Chem. Rev.* **1999**, *99*, 2161.
[20] M. Cossi, N. Rega, G. Scalmani, V. Barone, *J. Comput. Chem.* **2003**, *24*, 669.
[21] a) V. Barone, M. Cossi, J. Tomasi, *J. Chem. Phys.* **1997**, *107*, 3210; b) V. Barone, M. Cossi, *J. Phys. Chem. A* **1998**, *102*, 1995.
[22] F. Eckert, A. Klamt, *AIChE J.* **2002**, *48*, 369.
[23] a) P. Politzer, D. G. Truhlar, *Chemical Applications of Atomic and Molecular Electrostatic Potentials*, Plenum, New York, **1981**; b) S. R. Gadre, R. N. Shirsat, *Electrostatics of Atoms and Molecules*, Universities Press, Hyderabad, **2000**.
[24] a) C. H. Suresh, D. Ramaiah, M. V. George, *J. Org. Chem.* **2007**, *72*, 367; b) C. H. Suresh, S. R. Gadre, *J. Phys. Chem. A* **2007**, *111*, 710; c) K. V. Radhakrishnan, S. Anas, K. K. Syam, V. S. Sajisha, K. S. Anju, E. Suresh, C. H. Suresh, *New J. Chem.* **2007**, *31*, 237; d) C. H. Suresh, *Inorg. Chem.* **2006**, *45*, 4982; e) M. C. Basheer, S. Alex, U. Santhosh, V. Biju, C. H. Suresh, K. G. Thomas, S. Das, *Tetrahedron*, **2007**, *63*, 1617; f) C. H. Suresh, N. Koga, S. R. Gadre, *J. Org. Chem.* **2001**, *66*, 6883; g) C. H. Suresh, N. Koga, S. R. Gadre, *Organometallics* **2000**, *19*, 3008; h) S. P. Gejji, C. H. Suresh, L. J. Bartalotti, S. R. Gadre, *J. Phys. Chem. A*, **1997**, *101*, 5678; i) C. H. Suresh, S. R. Gadre, S. P. Gejji, *Theor. Chem. Acc.* **1998**, *99*, 151.
[25] A. C. Limaye, S. R. Gadre, *Curr. Sci.* **2001**, *80*, 1296.
[26] We have also optimised the structures of transition states **TS1** and **TS2** by using the basis set 6-31+G(d,p) consisting of the polarisation and diffused functions at the B3LYP level. These structures were very similar to the B3LYP/6-31G(d) level structures and the activation free energy values were nearly unchanged. Further, the **TS1** geometry showed only minor structural changes when optimised with PCM at the B3LYP/6-301G(d) level. See the Supporting Information for more details.
[27] a) T. Helgaker, E. Uggerud, H. J. A. Jensen, *Chem. Phys. Lett.* **1990**, *173*, 145; b) E. Uggerud, T. Helgaker, *J. Am. Chem. Soc.* **1992**, *114*, 4265; c) K. Bolton, W. L. Hase, G. H. Peshlherbe, in *Modern Methods for Multidimensional Dynamics Computation in Chemistry* (Ed.: D. L. Thompson), World Scientific, Singapore, **1998**, 143.

Received: February 9, 2008
Published online: May 8, 2008

